Construction and Building Materials

Effects of paraffin additives, as phase change materials, on the behavior of a traditional lime mortar

--Manuscript Draft--

Manuscript Number:	CONBUILDMAT-D-22-07515R1
Article Type:	Research Paper
Keywords:	Phase change material; lime mortar; Durability; Physical Properties; heat flux
Corresponding Author:	Jorge Feijoo | Feijoo-Conde, PhD Defense University Centre at Spanish Naval Academy SPAIN
First Author:	Jorge Feijoo | Feijoo-Conde, PhD
Order of Authors:	Jorge Feijoo | Feijoo-Conde, PhD
	M.A. Alvarez-Feijoo, PhD
	Rafael Fort, PhD
	Elena Arce, PhD
	Duygu Ergenç, PhD
Abstract:	This study refers to the inclusion of phase change materials (PCMs) in porous building materials as an alternative means of improving their thermal behavior, assessing the changes caused in their physical-mechanical and durability properties. Specifically, an organic paraffin wax was selected for direct incorporation into lime mortars using different concentrations by weight. The results show that PCMs improve the thermal properties of the mortar while reducing its accessible porosity. This increases the mortars' resistance to water and soluble salts. However, excessive PCM content causes stresses within the mortar that can jeopardize its structure.
Suggested Reviewers:	L.M. Ottosen, PhD Technical University of Denmark lo@byg.dtu.dk specialist in studies related to the improvement of mortar properties
	T. Rivas, PhD University of Vigo trivas@uvigo.es specialist in studies related to the enhancement of treatments used in heritage conservation
	M.J. Varas-Muriel, PhD Complutense University of Madrid mjvaras@ucm.es Specialist in the study of lime mortars, especially in the compatibility of certain additives.
	Mauro F. La Russa, PhD University of Calabria mlarussa@unical.it Specialist in the field of restoration, especially in the influence of nano additivation on the properties of building materials.
	Nevin Aly, PhD Suez University nevin.aly@suezuniv.edu.eg Specialist in the field of restoration with several papers on lime mortars

- Direct incorporation of an organic PCM in lime mortar was used
- PCM reduces accessible porosity and increases mechanical strength
- PCM improves mortar durability against water and soluble salts
- PCM improves the thermal properties of the mortar.
- Excessive PCM content has a negative effect on the mortar structure.

Graphical Abstract

The buildings sector has accounted for almost 35% of total global energy consumption for this reason a significant improvement in the energy efficiency of the sector is crucial.

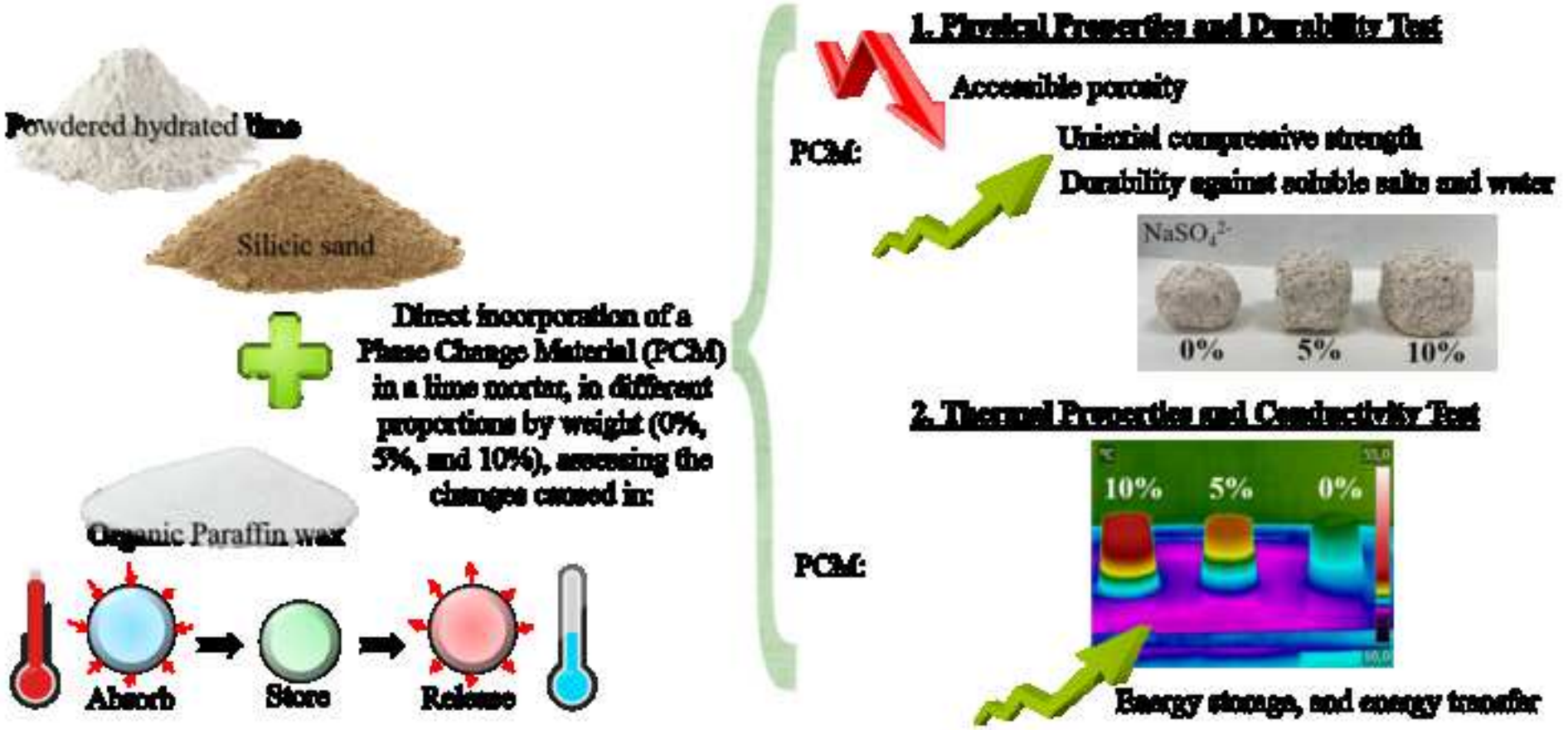

CRediT authorship contribution statement

J. Feijoo: Conceptualization, Methodology, Data curation, Formal analysis, Investigation, Writing - original draft, Supervision, Visualization, Funding acquisition. **M.A. Alvarez-Feijoo**: Conceptualization, Resources, Investigation, Writing - original draft, Supervision. **R. Fort**: Formal analysis, Writing - Review & Editing, Funding acquisition. **E. Arce**: Formal analysis, Writing - Review & Editing. **D. Ergenç**: Formal analysis, Writing - Review & Editing.

Effects of paraffin additives, as phase change materials, on the behavior of a traditional lime mortar

J. Feijoo*

Ph.D. Defense University Center, Spanish Naval Academy, GECYSE group, Plaza de España, s/n, Marín, 36920, Spain. jfeijoo@cud.uvigo.es ORCID 0000-0003-3820-5127

M.A. Alvarez-Feijoo

Ph.D. Defense University Center, Spanish Naval Academy, GECYSE group, Plaza de España, s/n, Marín, 36920, Spain. alvarezfeijoo@cud.uvigo.es ORCID 0000-0003-3027-075X

Rafael Fort

Ph.D. Institute of Geosciences IGEO (CSIC-UCM), c/Doctor Severo Ochoa, 7, 28040, Madrid, Spain. rafael.fort@csic.es ORCID 0000-0001-9967-2824

Elena Arce

Ph.D. Department of Industrial Engineering, University of A Coruña, CTC, CITIC, Ferrol, A Coruña, Spain, elena.arce@udc.es ORCID 0000-0001-7222-7827

Duygu Ergenç

Ph.D. Department of Civil Engineering, Middle East Technical University, Ankara, Turkey. dergenc@metu.edu.tr ORCID 0000-0001-9034-1818

* corresponding author

Abstract:

This study refers to the inclusion of phase change materials (PCMs) in porous building materials as an alternative means of improving their thermal behavior, assessing the changes caused in their physical-mechanical and durability properties. Specifically, an organic paraffin wax was selected for direct incorporation into lime mortars using different concentrations by weight. The results show that PCMs improve the thermal properties of the mortar while reducing its accessible porosity. This increases the mortars' resistance to water and soluble salts. However, excessive PCM content causes stresses within the mortar that can jeopardize its structure.

Keywords: phase change material; lime mortar; durability; physical properties; heat flux

1. Introduction

The buildings sector has accounted for almost 35% of total global energy consumption and 38% of total global energy-related CO_2 emissions since 2018 [1]. Furthermore, buildings' electricity consumption represents nearly 55% of the global total. This sector cannot be oblivious to climate change, one of the great challenges facing society today, since it makes a huge contribution to global energy consumption and greenhouse gas emissions. To achieve a net-zero-carbon building stock by 2050, the International Energy Agency estimates that both direct building CO_2 emissions and buildings' energy consumption must decline by 50% [2]. A significant improvement in the energy efficiency of the sector is therefore crucial, especially as regards increasing buildings' thermal efficiency to reduce heating and cooling needs.

This improvement in modern buildings' thermal efficiency, achieved, among other solutions, by installing ventilated facades or facades with external thermal insulation systems (SATE), is not considered a technical challenge today [3]. However, in buildings catalogued as cultural heritage, improving thermal efficiency is more challenging due to the impossibility, on either technical, legal, or esthetic grounds, of increasing the thickness of the facades.

One of the principal ways of decreasing indoor climate control requirements in recent years has been to include phase change materials (PCMs) in the construction materials. These materials have a high latent heat storage capacity, allowing them to store more energy than typical building materials [4]. They undergo a melting process, absorbing part of the solar heat (via an endothermic process during the phase change from solid to liquid) before subsequently releasing it into the environment when the outdoor or indoor temperature falls and the PCM solidifies (via an exothermic process during the phase change from liquid to solid) [5,6].

The wide variety of PCMs can be sorted into three main groups: inorganic, organic and eutectic materials [7,8]. Each of them has a series of advantages and disadvantages that will influence their final application [9,10].

Among the inorganic substances, hydrated salts are the most important because of their greater volumetric storage density (≈350 MJ/m^3) and relatively greater thermal conductivity (≈ 0.5 W/m·K) than organic materials [9,11]. However, the volume changes that these substances can undergo [8], as well as the damage caused by the more soluble salts—due to the pressures they exert on the pore-walls of a material when subjected to periodic crystallization/dissolution cycles [12,13]—discourage their use in certain applications, such as direct application in ornamental rocks. In fact, one of the greatest

and most difficult-to-solve forms of damage to building materials is the physical damage caused by soluble salts (such as sodium chloride or sodium sulfate) [14,15].

Organic PCMs, however, do not cause as high stresses as hydrated salts, as with organic consolidating and water-repellent compounds they can modify the pore structure of the material and accordingly modify other properties such as vapor permeability [16]. These changes may cause the treated material to become more prone to future damage since blockage of superficial pores can hinder water evaporation, tending to cause the salts that remain in the stone to precipitate below the treated surface [17].

In short, before applying this type of material to building materials, either by impregnating surfaces [18], encapsulation [19,20], absorption by immersion or by capillarity [21], direct incorporation into the porous materials as additives [22,23], or even by electroprecipitation techniques [24,25], a thorough study must be carried out to analyze the influence of the PCMs used on the materials' behavior, especially in properties related to the pore structure of the material. Consideration must be given to the fact that building materials, once put into service, are subject to the combined action of various deterioration agents, such as water or soluble salts. These agents can trigger both physical and chemical alterations that can jeopardize the durability of the construction if the correct treatment is not selected.

In the particular case of inclusion of PCMs as additives in mortars, the results obtained vary widely, thus demonstrating the influence that parameters such as the type of PCM used, the type of binder, the method of addition, and the dosages used in the mixture, among others, have on the final behavior of the mortar.

Lucas, Ferreira and Barroso de Aguiar [26] studied how the addition of microencapsulated paraffin as a PCM (Micronal DS 5008) influenced the mechanical behavior of mortars made of different binders. This study found that the incorporation of

PCMs in lime and lime-cement mortars resulted in an increase in their mechanical properties—with these increasing as the PCM dosage rose—since it caused a reduction in macroporosity. However, in cement mortars the effect was the opposite even though the changes in the pore structure of the untreated mortar were similar when a PCM was added.

Ventola, Vendrell and Giraldez [27] assessed the mechanical behavior of a lime mortar with different dosages of a microencapsulated PCM (Micronal DS 5001) and found that its addition increased uniaxial compressive strength (UCS) due to the increase in the porosity and pore size of the mortar, thereby favoring a higher degree of carbonation.

Kulkarni and Muthadhi [23] assessed the direct incorporation of different PCMs, both inorganic and organic, in a cement mortar, finding that incorporating inorganic PCMs reduced UCS by less than incorporating organic PCMs.

Lecompte *et al*. [28] analyzed how incorporation of a microencapsulated paraffin as a PCM (n-octadecane, C18H38) influenced the properties of concrete and cement mortars and found that the presence of this PCM reduced the UCS since the microcapsules behaved more like voids (with no significant effect on tensile strength) than common aggregates.

In a study published in 2014, Cunha [29] shows the influence of two different PCMs on the physical properties of lime-gypsum mortars, demonstrating that the characteristics given to the mortar differ depending on the polymer of the microcapsules. In studies conducted in 2015 [30] and 2016 [31], Cunha found that the addition of PCM microcapsules decreased the mechanical strength of different mortar types made with different binders (such as cement, gypsum, and hydraulic lime) due to the higher water content and, consequently, the higher porosity compared to the reference mortar. In a recent paper (published in 2020 [32]), Cunha found that although the direct addition of a

PCM reduced the capillary absorption capacity and increased the density of a cement mortar, the UCS was reduced at PCM contents higher than 10%, probably because PCMs were incorporated into the mixture in a liquid state, a parameter that affects porosity.

Cunha points out that the cost of construction materials dosed with encapsulated PCMs is almost seven times higher than that of non-encapsulated PCMs [32,33]. For this reason, and even though most published studies focus on the incorporation of encapsulated PCMs into construction materials, it is important to reduce the cost of incorporation in order to improve the applicability of this technology. Consequently, studies focusing on direct incorporation techniques, which remain an underdeveloped subject, are required.

The aim of this study is to analyze in detail the influence of direct incorporation of an organic paraffinic PCM on the physical-mechanical and thermal properties of a lime mortar. Although this mortar type, widely used in restoration of cultural heritage, is not as well studied as cement mortar, in recent years it has come back into use because it is more compatible (since, among other advantages, it is less rigid and does not contribute soluble salts to adjacent materials such as calcium sulfates and sodium salts [34,35]).

2. MATERIAL AND METHODS

2.1. Mortar: materials and preparation

Powdered hydrated lime (CL-90-S [92% $Ca(OH)_2$ and less than 5% MgO], provided by Calcinor) compliant with the UNE-EN 459-1 standard [36] and with a bulk density of 640 kg/m^3 was used as binder. Silicic sand (90% SiO_2), with the granulometric distribution curve shown in Figure 1 and with a bulk density of 1620 kg/m^3, was used as aggregate. This aggregate meets the ASTM C-144 standard [37].

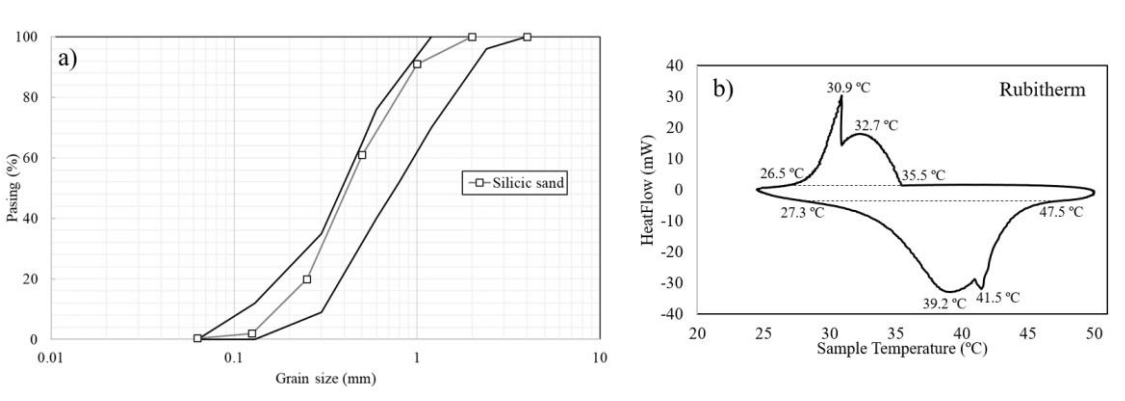

Figure 1. The graph on the left shows the grain size distribution of the aggregate used (the limits established by ASTM C-144 [37] are indicated by black lines). On the right is the differential scanning calorimetry of the PCM used, Rubitherm RT 35 HC (n = 3).

Rubitherm PCM RT 35 HC was used as additive. According to the manufacturer's data sheet, the properties of this organic paraffin wax are as follows: melting point 35 °C, density 880/770 kg/m^3 (solid/liquid respectively), specific heat capacity 2 kJ/kg·K, volumetric heat capacity 1760 kJ/m^3·K, latent heat of fusion 240 kJ/kg, and volumetric latent heat capacity 211 MJ/m^3. This PCM was chosen because it is a non-corrosive and chemically inert material with low thermal conductivity (0.2 W/m·K, for both phases), which favors its use as an insulating material. Before applying the PCM, this was characterized using differential scanning calorimetry (DSC). The raw PCM was heated from 20 °C to 50 °C at a rate of 5 °C/min in an N_2 atmosphere. Measurements were taken in triplicate using powder samples. The curves show the existence of a wide double peak, due to the PCM's organic nature [38], in both the freezing and the melting phases (similar behavior to that observed in other organic PCMs such as n-Butyl Stearate and Polyethylene Glycol [23]). The freezing temperatures ranged between 26.5 and 35.5 °C, peaking at 30.9 °C (Figure 2), which differs slightly with the value stated on the manufacturer's data sheet, which lists 35 °C as the maximum temperature. This range is

between 18 °C and 40 °C, which is considered the optimum PCM temperature range for building applications [8]. The melting temperature is between 27.3 and 47.5 °C, peaking at 39.2 °C, which again is slightly different to the value stated on the data sheet. The results obtained using DSC analysis stated that RT35HC has a latent heat capacity (enthalpy) of 240.7 ± 0.8 kJ/kg and 239.6 ± 2.3 kJ/kg at cooling and heating, respectively (similar values to those indicated on the data sheet). A disadvantage of this PCM is its high volumetric expansion during phase change (12%), which could affect the substrate to which it is applied.

Three different lime mortars were assessed in this study: one, as a reference, with no phase change material in its composition (named PCM0) and using a binder:aggregate volume ratio of 1:3, which is the most common ratio cited in the literature [35]; and two additives with differing PCM percentages: 5% and 10% by weight with respect to the amount of binder (named PCM5 and PCM10, respectively).

The amount of water added to the mortar mixes was adjusted to give them adequate and similar workability and consistency according to the slump test using the Abrams cone [39].

The water content in each mixture was measured following the gravimetric method. For this purpose, three samples were taken for each type of fresh mortar. The samples were weighed and placed in an oven at 50 °C for 3 days, after which they were removed and reweighed. The water content (WC) was determined according to the following equation:

$$WC\ (\%) = 100 \cdot (Ww - Wd) / Ww \quad (1)$$

where Ww is the weight of the wet mortar and Wd is the weight of the dry mortar.

Specifically, the amount of water added to each mixture, according to the gravimetric method of analysis, was as follows: PCM0-15.8%, PCM5-16.0% and PCM10-16.1% of total blend.

2.2. Mortar physical properties and durability test

Each mortar blend was placed in a different plastic mold to obtain three different geometries (cubic, cylindrical, and conical). The samples were demolded after 7 days and left to cure under laboratory conditions for 28 days (RH 70% ± 23% and 20 ± 5 °C).

After this period of time, and using 10 cubic samples per mortar (5 cm each side, as per the standards), water accessible porosity (UNE-EN 1936:2007 [40], Equation 2), capillary absorption coefficient (UNE-EN 1925:1999 [41]), and capillary porosity, using the expression shown in [42] (Equation 3), were determined. In all these cases, the mortar samples were weighed at the different time intervals established by the standard, with the initial state corresponding to dry weight before saturation in water, achieved by complete immersion in water (in the case of the water absorption process to determine the accessible porosity, Equation 2), or by partial immersion in the case of capillary porosity.

$$P_{\text{accessible to water}}\,(\%) = 100 \cdot (Ws - Wd) / (Ws - Wh) \qquad (2)$$

where W_s is the weight of the sample when completely saturated in water after applying vacuum, W_d is the dry weight of the sample, and W_h corresponds to the hydrostatic weight.

$$P_{\text{capillary}}\,(\%) = 100 \cdot (Wa - Wd) / (Vs \cdot \rho) \qquad (3)$$

where Wa is the weight of the sample saturated by capillary absorption, W_d is the dry weight of the sample, Vs is the volume of the mortar sample used, and ρ is the density of water.

Mercury accessible porosity and pore size distribution were measured by mercury intrusion porosimeter (MIP) using a Micromeritics Auto Pore IV 9500. This porosimeter makes it possible to characterize a pore range with an access diameter of between 0.003 and 360 μm. Measurements were taken in duplicate using 1 x 1 x 2 cm samples extracted from the core of the mortar samples. Based on the data obtained, the tortuosity of the porous network (τ) was also determined using the expression taken from a previous study [43] in which the total mercury injected by intrusion is compared with the mercury content retained in the samples during the extrusion process.

$$\tau = V_{intrusion\ Hg} / (V_{intrusion\ Hg} - V_{extrusion\ Hg}) \quad (4)$$

Also, the following properties were measured after 28 days of curing, using cubic samples:

Ultrasonic pulse velocity (UPV) was measured using a Pundit CNS Electronics instrument fitted with transducers (1 MHz frequency and 11.82 mm diameter), the tips of which were covered with conductive plastic to ensure robust coupling between the transducers and the samples (previously dried to constant weight). Ten direct measurements were taken in each orthogonal direction. The two highest and the two lowest values were eliminated, taking the mean of the remaining six as the real value. From these data, the anisotropy index proposed by Guyader [44] was obtained.

$$dM(\%) = [1 - (2V_{pmin}/(V_{pmean} + V_{pmax}))] \cdot 100 \quad (5)$$

where V_{pmin}, V_{pmean}, and V_{pmax} correspond to the lowest, intermediate, and highest velocity values, respectively.

The mechanical robustness of the mortar was assessed using the drilling resistance measurement system (DRMS, Sint Technology). Single holes were made in two mortar samples per mortar type (without and with PCM), setting maximum total penetration

depth at 20 mm. Drill bits with a 3 mm diameter were employed at a rotation speed of 100 rpm and a penetration rate of 10 mm/min (conditions suitable for materials expected to have low resistance [45]).

The mortars' surface hardness was evaluated with the Equotip rebound tester (following ASTMD 5873 [46]) using an Equotip3 (Proceq) with a D-type impactor. Twelve downward measurements perpendicular to the surface of the dried mortar samples were taken (n = 10 per mortar type). The Equotip hardness value (Ls) was also used to predict the UCS using the expression proposed by Aoki and Matsukura [47].

$$UCS\ (MPa) = 0.079e^{-0.039 \cdot n} \cdot Ls^{1.1} \quad (6)$$

where n is the accessible porosity to water (in %) and Ls the Equotip hardness value.

The durability index of the three types of mortar was calculated using two mathematical estimators: the DDE proposed by Ordoñez [48], and the PDE_c proposed by Benavente [49]. Both estimators provide an idea of the durability of the material to the pressures exerted by salt crystallization and freeze–thaw cycles. The DDE estimator, which considers only the porous structure of the material, was calculated using the following expression:

$$DDE\ (\mu m^{-1}) = \Sigma(D_v(r_i)/r_i)P_a \quad (7)$$

where D_v is the pore size distribution for each pore r_i (in parts per unit); r_i the pore size in µm; and P_a the accessible porosity to water in parts per unit.

The PDE_c estimator, which improves on the previous one since it not only considers the porous structure of the material but also considers its mechanical strength, was determined by means of the following equation:

$$PDE_c\ (m/kg) = 10\ DDE/UCS \quad (8)$$

In both cases, the higher the value of each mathematical estimator, the lower the durability exhibited by the material.

Microstructure, morphology and chemical composition were studied by environmental scanning electron microscopy (ESEM) and energy-dispersive X-ray spectroscopy (EDX) using an FEI ESEM Quanta 200 microscope equipped with an EDAX EDX detector. Elements from polished sections were spatially distributed to obtain EDX elemental mapping images for each mortar. In addition, the images were processed with ImageJ software to highlight the intra-particle porosity.

Once the mortar samples' hardness had increased after 60 days of curing under laboratory conditions, the mortars' carbonation degree and durability were evaluated against different alteration agents.

Carbonation degree was determined using a thermogravimetry-differential scanning calorimeter (TG-DSC, Labys Evo 1180). For this purpose, two conical samples of each mortar type (height 9 cm, bottom and top diameters 6.3 cm and 4.3 cm, respectively) were divided along their longitudinal profile by means of hammer and chisel. On the exposed surfaces, the material was scraped and then ground, sieved, and dried before measuring. The measurements were taken in an N_2 atmosphere, heating the samples from 30 to 900 °C using a heating ramp of 10 °C/min. Carbonation degree was calculated from the relation between portlandite ($Ca(OH_2)$ depletion and, especially, calcite ($CaCO_3$) formation [33,50]). In addition, the carbonation degree was evaluated qualitatively by dying the longitudinal sections of the conical mortar samples—which had been divided in half—with phenolphthalein ($C_{20}H_{14}O_4$) to measure the carbonation depth.

Resistance to thermal cycles (UNE-EN 16140:2019 [51]) was determined in order to analyze whether continuous changes in the phase of the PCM within the mortar, as well as the different thermal expansion coefficients between the PCM and the lime mortar, can

cause internal stresses that trigger the appearance of fractures or loss of material. Each cycle consisted of oven-drying at 75 °C for 18 h, followed by total immersion in ultrapure water at 20 °C for 6 h. A total of 20 cycles were performed, using 3 cylindrical samples per mortar type (diameter 5.7 cm, height 12.2 cm). Every 3 cycles the samples were dried to constant weight to analyze the weight loss during the test.

Frost resistance (UNE-EN 12371:2011 [52]) was determined by evaluating the behavior of the mortar against freeze–thaw weathering processes exerted by water when it freezes and expands in volume. Each cycle consisted of 2 h of vacuum saturation with ultrapure water (conductivity of 0.054 µS/cm) to avoid the influence of the salts on the alteration process, freezing at -25 °C for 8 h, and defrosting in water at room temperature for 6 h (25 ± 2 °C). A total of 10 cycles were performed using 5 conical samples per mortar type (similar dimensions to those mentioned above). Every 2 cycles the samples were dried to constant weight and their weights were recorded.

Resistance to salt crystallization cycles (following the RILEM procedure [53] modified according to [54]) was determined using three different salts (single salts such as NaCl 20 w/w%, Na_2SO_4 14 w/w%, and a salt mixture: seawater) and 5 cubic samples (5 cm per side) per mortar type. Each cycle consisted of 2 h in total immersion in the corresponding saline solution, 4 h in an oven at 40 °C, and drying at 20 °C and RH 80% for 18 h. Every 5 cycles, the samples were desalinated by immersion in water for one week. After this process, the samples were dried until constant weight was reached.

The reason for selecting these salts was as follows: NaCl is a very common salt present in buildings, especially those located in coastal areas [55]. This salt, which has a high solubility and only has one stable phase, is mainly responsible for surface alteration processes such as sanding [56]. Na_2SO_4 is considered to be one of the most dangerous salts for building stone, causing the loss of material through superficial detachment [57].

The damage caused by this salt is attributed to both crystallization pressure and hydration pressure as its volume increases by 300% when it changes state from thenardite (Na_2SO_4, anhydrous) to mirabilite ($Na_2SO_4 \cdot 10H_2O$, decahydrated) [58]. Seawater was used to approximate the analyses to a real-world situation, since it is more common to find buildings affected by a combination of salts than by a single one [14,59,60]. The ionic composition (in % w/w) of the seawater used was as follows: Cl^- (1.94), SO_4^{2-} (0.27), Na^+ (1.1), Mg^{2+} (0.13), Ca^{2+} (0.04), K^+ (0.04). The seawater was similar to that used in [61].

Resistance to or durability against these alteration agents was measured as weight loss during the test. In addition, the degree of alteration was visually monitored.

2.3. Mortar thermal properties and conductivity test

Heat storage capacity and long-term stability were analyzed to determine both the heat storage capacity at fixed temperature intervals and the number of cycles that PCMs can withstand without suffering degradation of their properties. For this purpose, a TG-DSC was used to assess the change in behavior of the samples when subjected to a programmed temperature cycle in a controlled atmosphere ($N_{2(g)}$). Each cycle commenced by heating the sample from 20 °C to 50 °C using a heating ramp of 2 °C/min. Once this temperature was reached, it was maintained for 15 min to stabilize the sample temperature before returning it to 20 °C, cooling it at 2 °C/min. The samples were left at this temperature for 15 min to stabilize before starting the next cycle. A total of 80 cycles were performed per mortar type (i.e., PCM0, PCM5, and PCM10), conducting the analysis in duplicate.

Thermal conductivity under various conditions:

- Cold conductivity test. Three conical samples (height 9 cm, bottom and top diameters 6.3 cm and 4.3 cm, respectively) per mortar type were heated to 60 °C

in an oven. They were then partially immersed in water (previously cooled to 12 °C and 1 cm deep). Every 10 minutes, the temperature of the samples was recorded using a Flir E85 thermographic camera with an emissivity of 0.94 (recommended value for mortar- and limestone-type materials [62]), taking the corresponding photograph. The FlirTools+ software was used to determine both the temperature value at two predefined heights (2 cm and 5 cm from the base of the samples) and the immersion bath temperature.

- Hot conductivity test. In this case, other 3 conical samples per mortar, with the same dimensions as those of the previous test, were used. The samples were previously cooled in a freezer until they reached -17 °C. They were then partially immersed in water (at 35 °C and 1 cm deep). During the test, and at the same time intervals as in the previous test, the temperature was recorded, and the data were processed with the Flir E85 camera and its corresponding software.

3. Results and Discussion

3.1. Physical-mechanical properties

Table 1 shows the data on the main physical properties of the three mortars assessed in this study. The data show that:

The addition of a PCM to lime mortar results in an alteration in the physical properties of the mortar. The higher the PCM content in the mixture, the lower the accessible porosity of the mortar, both to water and to mercury. These results do not concur with those obtained in previous studies carried out on lime mortar [26,27], probably due to the fact that in those studies a greater amount of water was added to the mortars containing a PCM than in the reference mortar (this fact, as stated in previous studies, causes an increase in porosity [63,64]), while in this study the amounts of water added were very similar.

However, this result is in agreement with those obtained in [32], where the addition of a PCM to cement mortar was performed in the same way as in this study.

Table 1. Physical properties of the different mortars assessed, with and without PCM.

Parameters	**PCM0**	**PCM5**	**PCM10**
Water accessible porosity (% v/v)	37.06 ± 0.31	35.31 ± 0.16	33.97 ± 0.27
Mercury accessible porosity (% v/v)	30.10	22.93	21.84
Capillary porosity (% v/v)	28.28 ± 1.00	28.56 ± 0.22	28.06 ± 0.32
Capillary coefficient ($kg/m^2\ s^{0.5}$)	0.321 ± 0.016	0.321 ± 0.004	0.316 ± 0.004
Bulk density (kg/m^3)	1645 ± 8	1632 ± 6	1607 ± 8
Tortuosity	1.35	1.34	1.73
Ultrasonic pulse velocity (m/s)	1160 ± 23	1129 ± 1	1171 ± 0
dM (%)	3.50 ± 0.93	1.64 ± 0.85	1.17 ± 0.89
Surface hardness (Leeb, HLD)	201.72 ± 3.58	201.26 ± 2.72	211.63 ± 5.38
Uniaxial compressive strength (MPa)	6.39 ± 0.12	6.82 ± 0.10	7.59 ± 0.21
DDE (μm^{-1})	0.61	0.12	0.10
PDEc (m/kg)	0.95	0.17	0.14

Analyzing the pore size distribution (Figure 2), it was observed that the reduction in porosity is due to the filling of the smallest pores (under 1 μm) by the PCM, and to the partial occlusion of pores that, being found in the PCM0 mortar outside the detection range of the equipment (360 μm), appear at around 10 μm in the PCM-additivated mortars. This result is in agreement with those obtained in previous studies showing that the PCM produces a filling effect by reducing the porosity of the treated material [33,65]. The same result can be seen in Table 2, which shows the intruded volume in each mortar type for different pore size ranges.

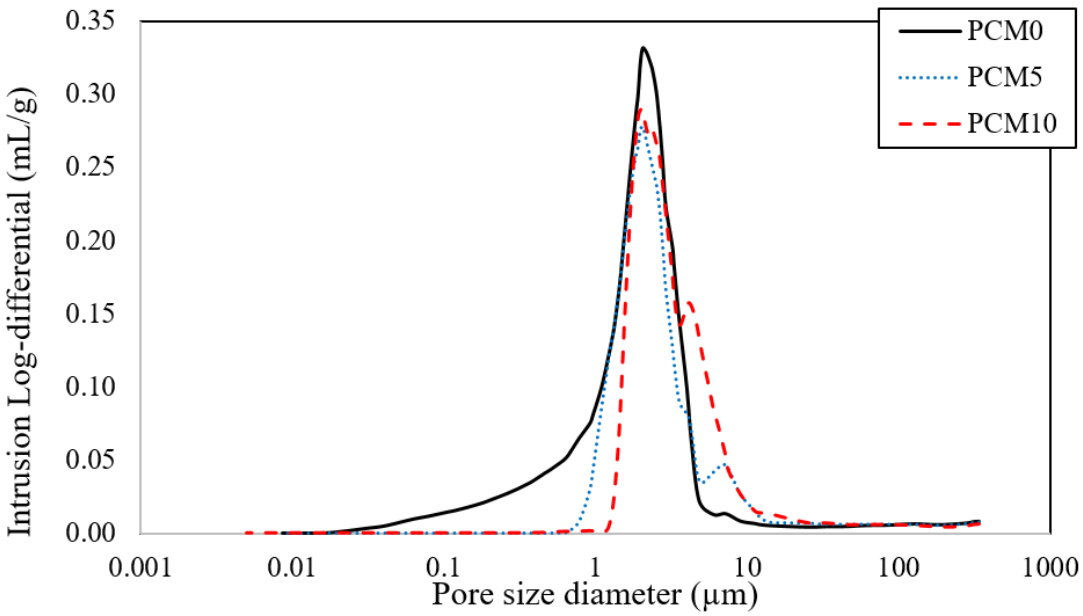

Figure 2. Average pore size distribution (n = 2) of the mortar samples, without a PCM (black line) and with different PCM percentages: PCM5 (dotted blue line) and PCM10 (dashed red line).

Table 2. Intruded mercury volumes for different pore size ranges (in %) for the three different mortars assessed: PCM0, PCM5 and PCM10.

Mortar	Mercury accessible porosity (% v/v)	Total intruded volume (%)				
		Pore size ranges (µm)				
		< 0.1	**0.1–1**	**1–10**	**10–100**	**> 100**
PCM0	30.10	2.51	19.21	73.75	2.69	1.84
PCM5	22.93	0.00	1.55	90.71	5.39	2.35
PCM10	21.84	0.00	0.30	92.13	5.77	1.80

This variation in porosity affects other properties, such as capillary suction capacity and pore network tortuosity. Capillary porosity and capillary coefficient barely changed in the mortar samples when the amount of PCM added was low (i.e., in PCM5; Table 1 and Figure 3a). However, when the amount of PCM added was high enough to occlude the pores measuring 0.1–1 µm (as happens in PCM10; Table 2), corresponding to the smallest range of pores with a capillary access size of 0.1–100 µm [66], a slight decrease occurred.

However, it should be noted that the results obtained were not statistically very different, considering the deviation of the measurements. What was really observed was the influence exerted by the PCM on the degree of saturation of the samples by this absorption mechanism (Figure 3b). As can be seen in Table 2, the pore volume in PCM mortars is mainly concentrated in that family of pores with an access size of 1–10 µm. The fact that they lack a lower accessible porosity and that most of the pores are within this range means that the degree of saturation of the mortar samples via this entrance route will be higher in mortars with a PCM, especially in the PCM10 mortar, which presents a degree of saturation by capillarity of 83%.

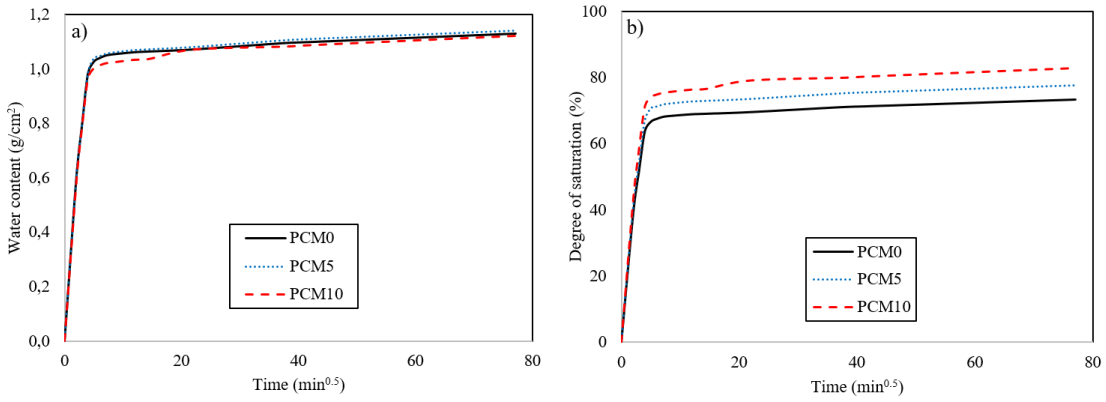

Figure 3. Water content per surface area as a function of time (in minutes) during the capillary absorption test (a). The degree of saturation (S%) absorbed by capillary suction as a function of time is also shown (b).

Concerning tortuosity, the inclusion of particles that occlude the smallest pores and partially fill the largest ones caused an increase in this property when the amount of PCM added was high (PCM10). This could be counterproductive, since, as indicated in [25], the greater tortuosity of the pore system hinders the transport of moisture during desorption, maintaining a higher residual moisture content in the material for a longer period of time.

The ultrasound pulse velocity measurements showed a slight increase in the PCM10 mortars, probably due to the lower porosity, as occurs in [25]. However, for low PCM concentrations (5%) this increase was not observed.

The anisotropy values detected were very low (less than 5%; Table 1), especially in the PCM-additivated mortars, so from a mechanical point of view these mortars can be considered, according to [67], isotropic materials.

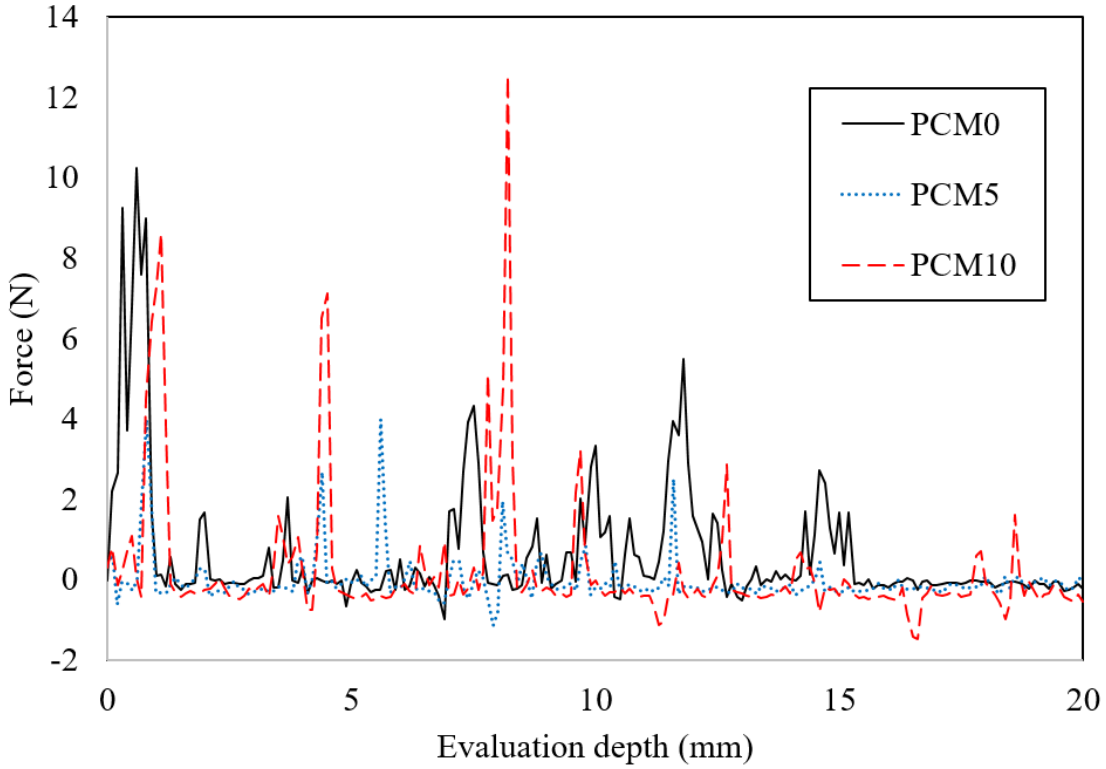

Figure 4. Measurement of drilling resistance expressed as the force exerted by the drill (in N) vs. evaluation depth in the cubic mortars (in mm), without and with PCM (n = 2).

Regarding drilling resistance, the PCM was not observed to cause a variation in the resistance of the reference mortar (Figure 4). On average, the resistance exerted by each of the three mortar types was very low and similar. Occasional peaks in strength were observed, which may be attributable to quartz grains as they also appear in the mortar

without PCM.

However, an increase was observed in the other two mechanical properties analyzed in this study. The impact resistance obtained using the microhardness tester showed how the addition of a high PCM content (in this case 10%) increased this property. Similarly, it can be seen that the addition of the PCM produced a slight increase in the uniaxial compressive strength of the reference mortar (increases of less than 2 MPa, which are similar to those obtained in [27], which evaluated the use of lime mortars with a PCM). The results show that the greater the PCM content added, the greater the UCS achieved. This is attributed, as indicated above when analyzing the porous system, to the reduction in the number of voids in the mortar section and in their size, which allows for greater compaction of the mechanically useful skeleton (see Figure 5, where the pores are highlighted in red). As occurs in other studies, a lower porosity causes an increase in UCS [26,68–70]. SEM images and mapping also show that no changes in mortar composition were observed.

The durability index against pressure exerted by water or soluble salts (i.e., DDE and PDEc) indicates that after 28 days the durability of the mortars increased with the amount of PCM content added to the mixture (Table 1). This fact is related to 1) the lower accessible porosity, which hinders the entry of external alteration agents; 2) the lack of small pores that are more prone to crystallization pressure, as stated in [71]; and 3) the greater mechanical resistance of these mortars [49].

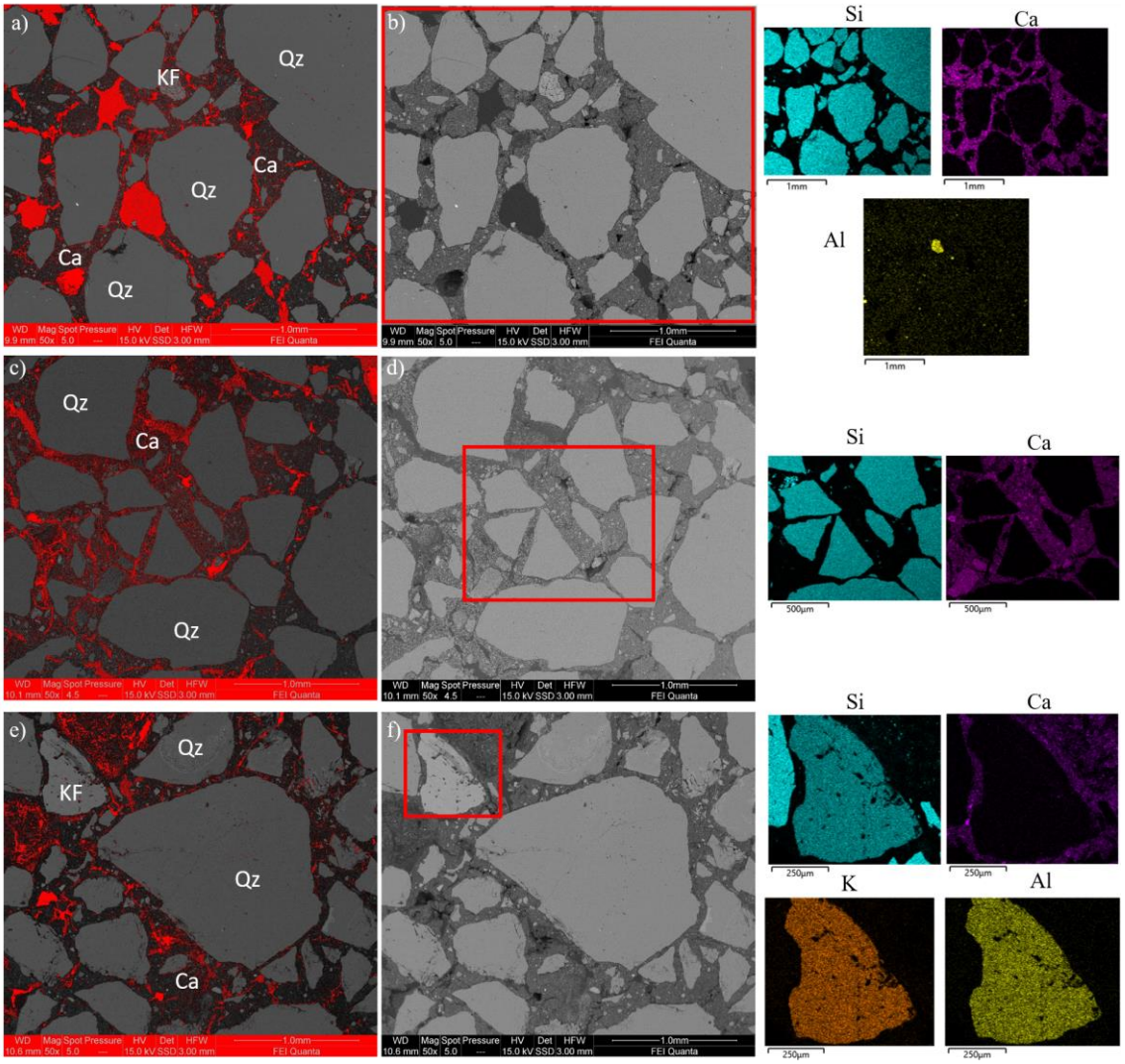

Figure 5. ESEM micrographs (cross-section) of the mortars assessed in BSE mode: PCM0 b), PCM5 d), and PCM10 f), and their corresponding EDX mapping. These micrographs and the EDX analyses show the typical mineral grains of the mortar composition: quartz grains (Qz) and potassium feldspar (KF) from the aggregate, and calcium carbonate (Ca) from the binder. In addition, the intergranular porosity details can be observed in the processed images: PCM0 a), PCM 5 c), and PCM10 e).

Carbonation measurements taken at 60 days indicated that the degree of carbonation was reduced with the addition of the PCM (Figure 6), a similar result to that obtained in [33]. This is evident from both thermogravimetric and phenolphthalein results. In the

thermogravimetric analysis three weight-loss zones were observed: one between 200 and 300, which is associated with the flash point of the paraffinic PCM; other between 350 and 450 related to the dehydration of calcium hydroxide; and a final one between 500 and 850 related to the decomposition of calcium carbonate [72]. The results show that the highest loss associated with calcium carbonate and the lowest loss associated with the presence of $Ca(OH)_2$ occur in the PCM0 mortar. Meanwhile, the greatest loss associated with the PCM occurs in the PCM10 mortar.

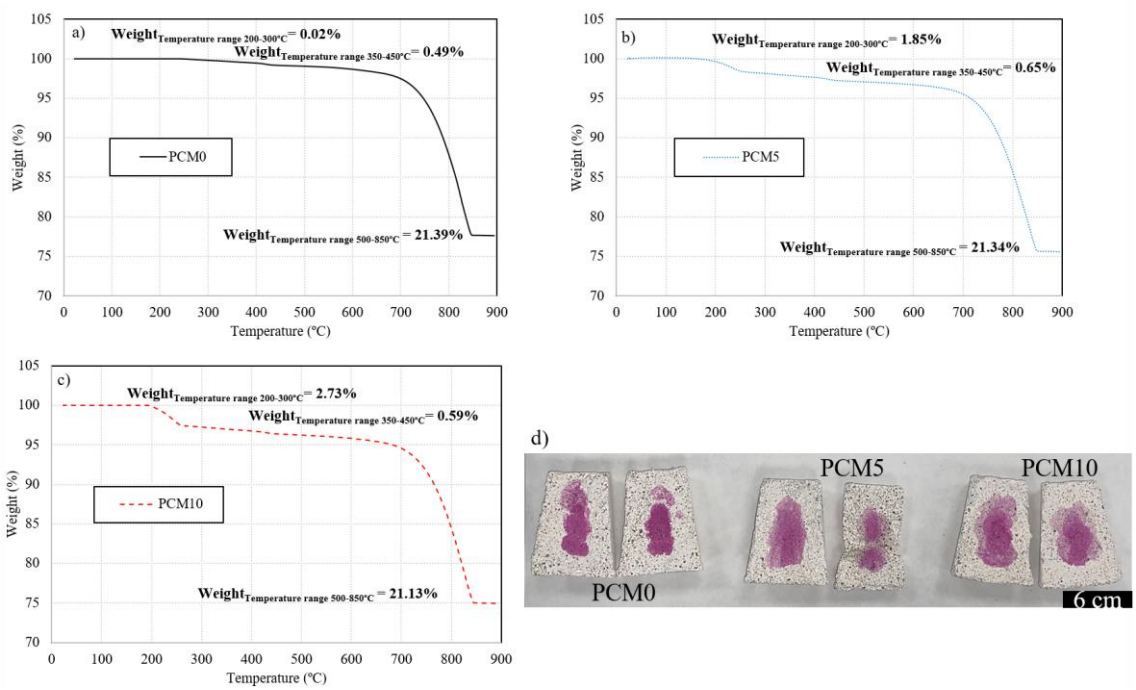

Figure 6. Thermograms corresponding to each of the mortars assessed (PCM0 [a], PCM5 [b], and PCM10 [c]), showing the average percentage weight loss (n = 2) at different temperatures. A longitudinal section dyed with phenolphthalein to measure carbonation depth is also shown (the uncarbonated areas are shown in pink).

The lower carbonation of the PCM10 samples—followed by the PCM5 samples and found especially in the core of the samples (Figure 6d)—is related to the greater difficulty the CO_2 encounters in flowing through the mortar matrix (an essential factor for

carbonation to take place, as mentioned in [73]). As mentioned above, the PCM10 mortar has a lower accessible porosity and a greater tortuosity than the other two mortars (Table 1). This lower degree of carbonation depth in the samples containing the PCM has a negative influence on the UCS, as demonstrated in [74,75]. Therefore, if the degree of carbonation depth were similar, the difference observed in the UCS between the PCM-additivated mortar and the reference mortar would be much greater.

3.2. Resistance to external alteration agents

Figure 7 shows the average weight loss for each mortar type measured during the thermal cycles to which the samples were subjected. The obtained results showed that the highest weight losses occurred in the PCM10 mortar (14% at 20 cycles). In this mortar type, the development of small fractures, which would enlarge until reaching the size shown in the attached photograph, began in cycle 12. The next mortar type with the highest loss was the PCM5 mortar (around 8% at 20 cycles), which developed small fractures in the corners of the samples. In the PCM0 mortar, neither weight loss nor fractures were observed. The development of these fractures is related to the internal stresses generated by the PCM within the mortar matrix due to mismatching of the coefficients of thermal expansion between the two materials: lime mortar (the value of which is usually around 2.5%, as stated in [76]), and the selected PCM (RT 35 HC: 12%).

As shown in previous studies that analyze the damage caused by the different thermal expansion coefficients between soluble salts [77] or PCMs [78] and the matrix of the porous materials, the damage is greater 1) when the porous material presents a higher concentration of these compounds (i.e., soluble salts or PCM content); and 2) when the crystal practically fills the interior of the pore. Both facts are consistent with the results obtained in this study, where it can be seen how the inclusion of a PCM tends to fill the

smaller pores (Figures 2 and 5) and that the damage is greater in the mortar with 10% PCM content.

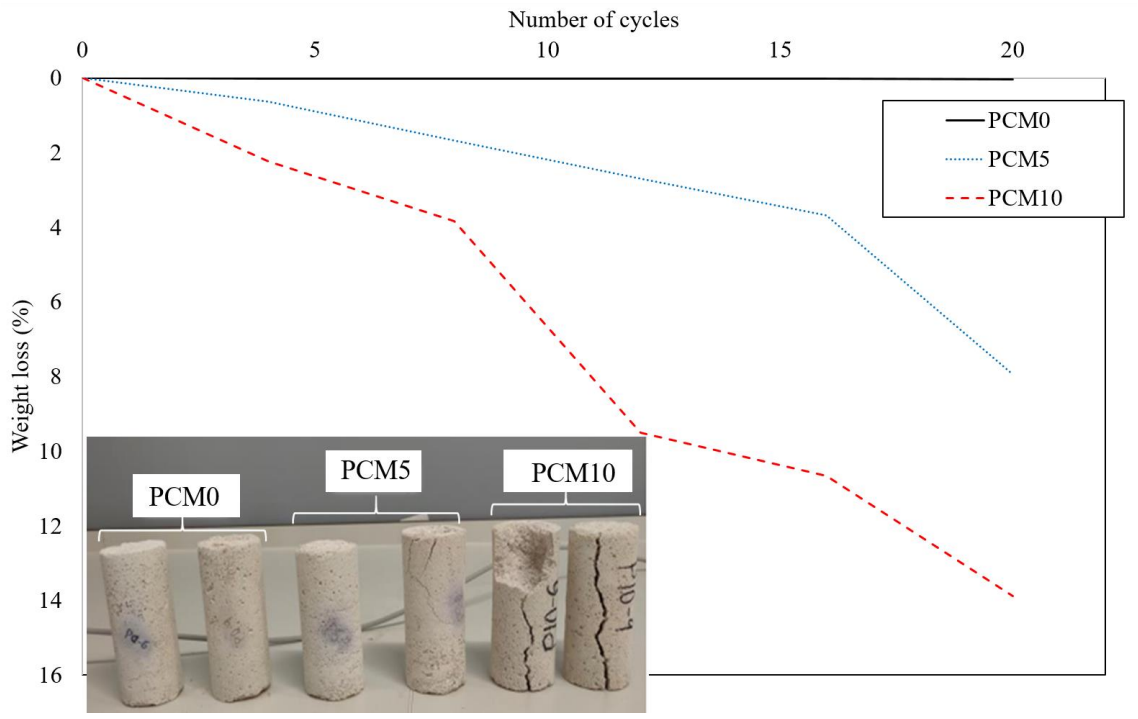

Figure 7. Average weight loss in % (n = 3) suffered by the mortars as a function of the number of thermal cycles performed. In addition, the final state of some of the samples used in the test is shown once the 20 cycles have been completed.

Regarding the resistance to freeze–thaw cycles (Figure 8), the result was the opposite of the previous one. In this case, the greatest weight loss occurred in the reference mortar (PCM0, 40% after 10 cycles, resulting in the loss of the mortar samples' shape) and was lower in the mortars with PCM additives (less than 0.6%, regardless of the amount of PCM added). Fractures in mortar PCM0 were observed from the 5th cycle onwards. Summarizing, the absence of pores smaller than 1 μm, as occurs in PCM mortars, gives the mortar a better capacity to absorb the expansive pressures generated by the increase in volume that occurs when the water changes from liquid to solid state, as stated in [13].

In addition, this resistance is enhanced by the reduction in accessible porosity, which means that less water can penetrate the mortar.

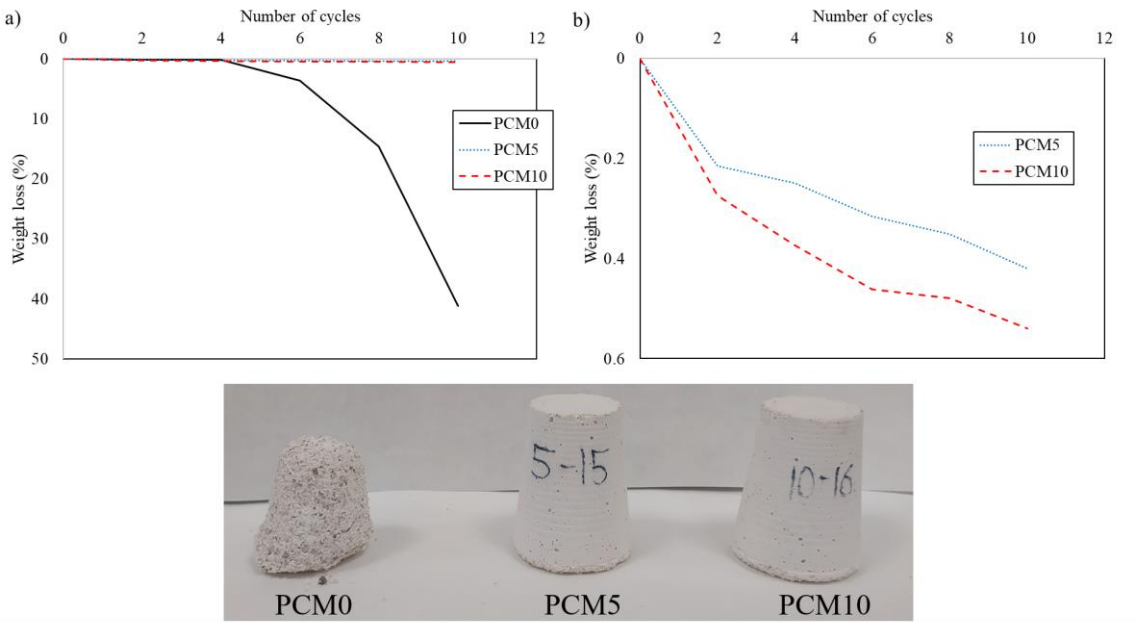

Figure 8. Average weight loss in % (n = 3) suffered by the mortars as a function of the number of freeze–thaw cycles performed (on the right is shown in detail the weight loss suffered in PCM mortars). The final state of some of the samples used in the test once the 10 cycles had been completed is also shown.

Finally, Figure 9 shows the weight loss suffered by the three mortar types when subjected to alteration processes with different types of salts. The obtained results show that, regardless of the salt used, the PCM-additivated mortars behaved similarly and exhibited greater resistance than mortar samples without PCM. This is due, as was the case in the freeze–thaw cycles, to the change in the pore structure of the lime mortar, and in the accessible porosity (Table 1 and Figure 2), caused by the addition of the PCM. Given that crystallization pressure is inversely proportional to pore size [71,79], the disappearance of small pores results in lower crystallization pressure in these materials. Visually, it was

observed that the greatest loss of material occurred in the PCM0 mortars, which lost their shape. Among each of the salts used, and as would be expected, the greatest losses occurred with sulfate alteration, followed by sodium chloride and, to a lesser extent, seawater alteration.

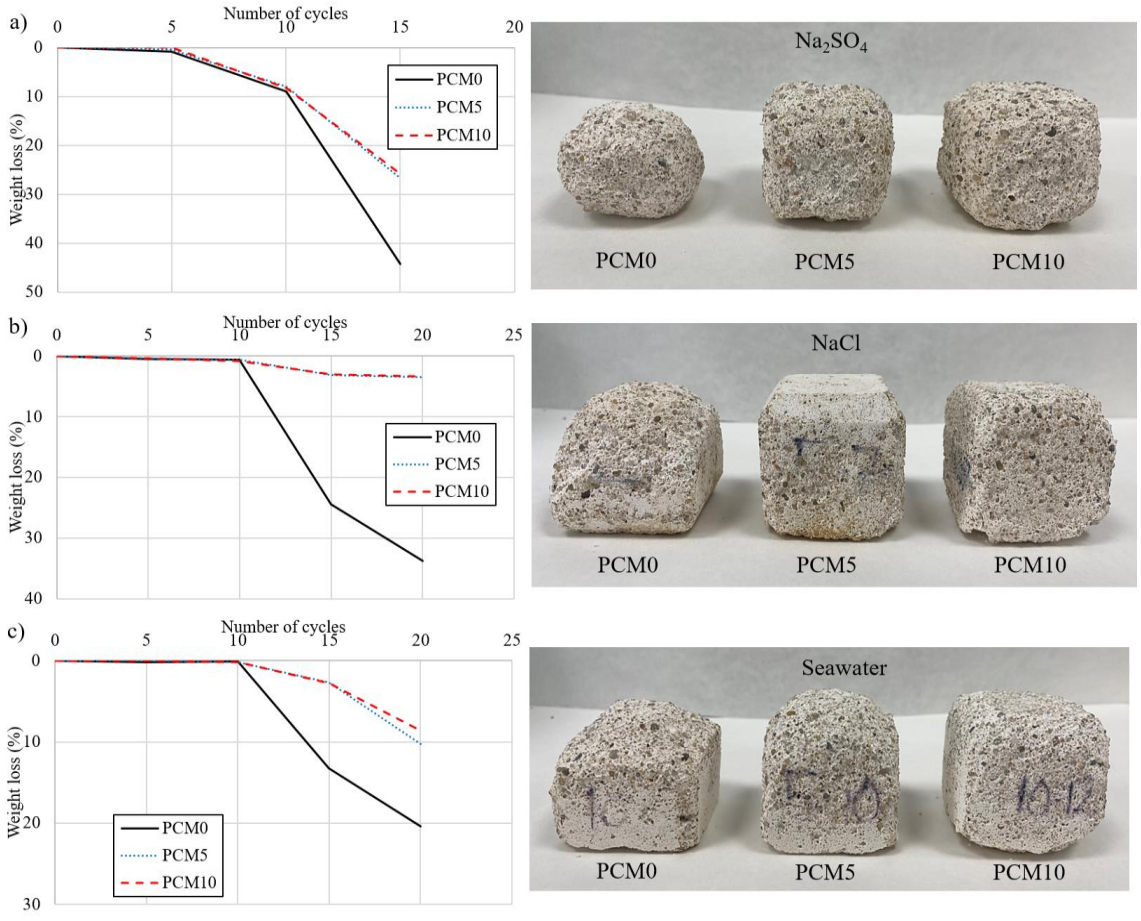

Figure 9. Average weight loss in % (n = 5) during salt crystallization cycles using Na_2SO_4 (a), NaCl (b), and seawater (c) on different mortars: PCM0 is represented by the straight black line, PCM5 by the dotted blue line, PCM10 by the dashed red line. Macroscopic images of several mortar samples obtained at the end of the respective crystallization cycles are also shown.

As can be seen, the PCM-additivated mortars' greater resistance at 60 days to the action of soluble salts and water is similar to that already indicated by the mathematical estimators DDE and PDE_c at 28 days.

3.3. Thermal properties

Figure 10 shows the heat fluxes corresponding to the temperature cycles performed on each mortar type. From the obtained results, it can be seen that the addition of the PCM improves the thermal properties—with regard to heat retention and heat transfer capacity—of the mortar without the PCM, especially as the content of this compound increases in the blend, a similar result to that reported in [23,80]. In general, it was observed that there was no variation of heat flow in the PCM0 mortar. In other words, it remained practically constant despite the variation in temperature. As the PCM was added, the peaks characteristic of the raw PCM used (Figure 1) began to appear during both the melting and freezing phases. In the PCM5, the latent heat capacity reached 1.7 ± 0.04 kJ/kg and 1.7 ± 0.05 kJ/kg in the cooling and heating phases, with the freezing and melting points being 34.9 °C and 30.7 °C, respectively. With an addition of 10% PCM (i.e., PCM10) a double peak in the freezing phase (at 33 °C and 36 °C, approximately) and a single peak in the melting phase (at 35.7 °C) were observed. The latent heat capacity achieved in this mortar was almost twice that achieved in PCM5 (4.1 ± 0.07 kJ/kg and 3.9 ± 0.02 kJ/kg during the freezing and melting phases, respectively). This fact does not mean that the addition of a certain PCM content leads to a proportional increase in latent heat.

As might be expected, and as occurs in other studies [63], the thermal behavior observed in the PCM-additivated mortars—in terms of temperature peaks in melting and freezing phases—differs from that shown by the raw PCM (Table 3). This difference decreases as more PCM is incorporated into the mixture.

Table 3. Summary of DCS results obtained for the raw PCM (RT 35 HC) and the mortars with the PCM in their composition (PCM5 and PCM10).

	Melting phase		Freezing phase	
Specimen	**Peak Temp. (°C)**	**Latent Heat Capacity (kJ/kg)**	**Peak Temp. (°C)**	**Latent Heat Capacity (kJ/kg)**
RT 35 HC	39.2	239.6	30.9	240.7
PCM5	30.7	1.7	34.9	1.7
PCM10	35.7	3.9	32.8	4.1

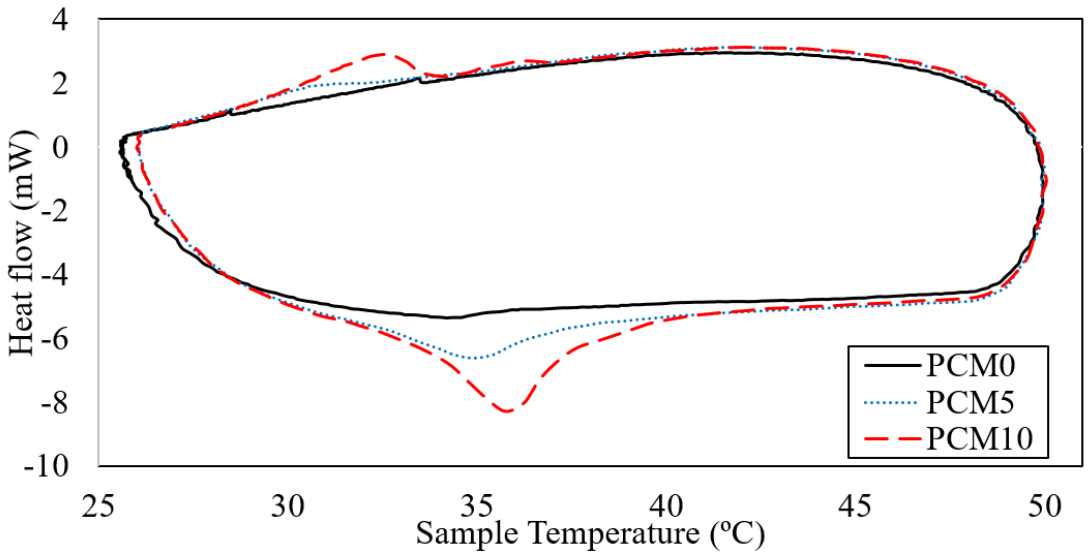

Figure 10. DSC analysis of mortars with differing PCM content: 0% (PCM0, straight black line, 5% (PCM5, dotted blue line), and 10% (PCM10, dashed red line).

Regarding the stability of the mortar mixtures after 80 cycles (Figure 11), it can be observed that in all cases, regardless of the PCM content, there was not much variation in heat flow, with different cycles showing similar melting and freezing points.

Figure 12, which corresponds to the cold conductivity test, shows the temperature variation recorded in both the upper and lower parts of the mortar samples after heating them to 60 °C then placing them in water at 12 °C. In general, it was observed that samples containing the PCM took longer to cool than samples without the PCM, which reached the water temperature much earlier. This result is related to the mortar's capacity to store energy when the PCM's melting point (in this case 39 °C) is exceeded, and to release it when the temperature decreases below the freezing point (in this case approximately 31 °C). For both the PCM5 and PCM10 mortars, at 31 °C (the PCM phase change temperature) there is a slowdown in temperature loss (lower slope of the curve). This slowdown is more pronounced when PCM content is higher (i.e., in the PCM10 mortar samples) due to the greater latent heat absorbed and subsequently released by this mortar (similar result to that achieved in [23]). Thus, it was observed that at 50 minutes the samples without the PCM reached the water temperature throughout their mass, while in those with the PCM the time increased to 80 and 150 minutes for the PCM5 and PCM10 mortar samples, respectively. This result is similar to that obtained in previous studies, where it was evident that the addition of the PCM improved the thermal behavior of the material [4,27].

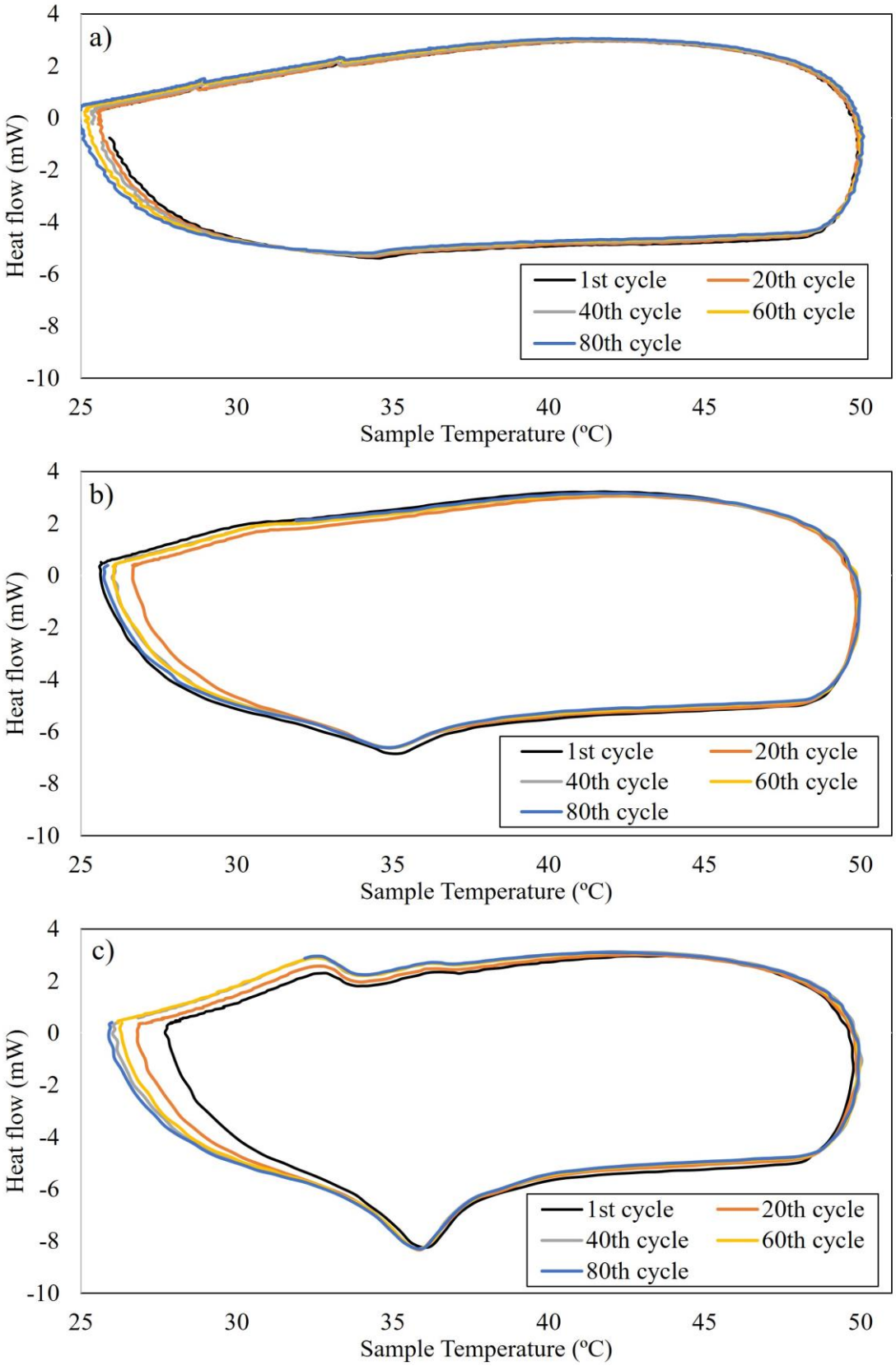

584

585 **Figure 11.** DSC analysis for the PCM0 (a), PCM5 (b), and PCM10 (c) mortars over 80

586 thermal cycles.

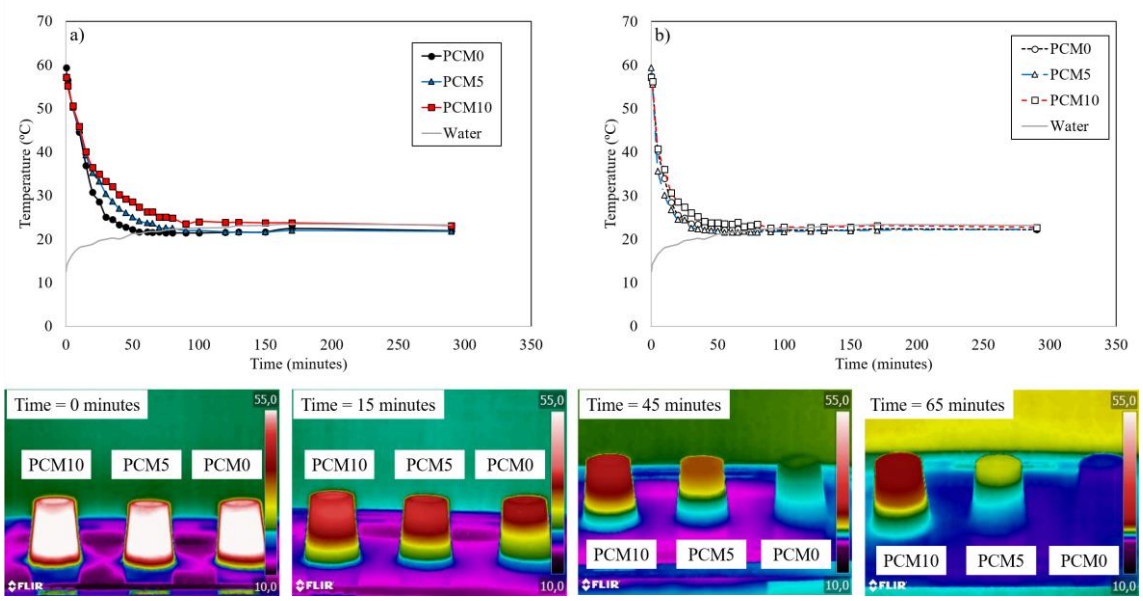

Figure 12. Average temperature variation (n = 3) recorded at heights of 5 cm (a) and 2 cm (b) above the base of the mortar sample during the cold conductivity test, as well as the average temperature variation of the water in contact with the samples. Thermal images of the front sides of the mortar samples, both without and with PCM, at different time intervals are also shown.

Regarding the opposite test where cold mortar samples were placed in hot water (hot conductivity test, Figure 13), it was observed that the PCM10 samples reached the water temperature earliest, regardless of recording height. They were followed in order by the PCM5 and PCM0 samples. In this test, the melting point of the PCM was not reached, which avoided its melting, so the results obtained are attributed to a conjunction of the following factors related to the properties of the mixture: 1) the higher thermal conductivity of the added PCM (0.2 W/m·K) compared to air (0.02W/m·K), which favors thermal diffusivity [81]; 2) the lower porosity of the PCM-additivated mortars compared to PCM0, since a reduction in porosity will increase the thermal conductivity and thermal diffusivity of the mixture [81]; and 3) the higher degree of capillary saturation reached

by the PCM-additivated mortars, especially the PCM10 samples, and the non-existence of pores smaller than 0.1 µm that are not accessible to water (Figures 2 and 3), which produces earlier thermal equilibrium between the mortar and the water [82].

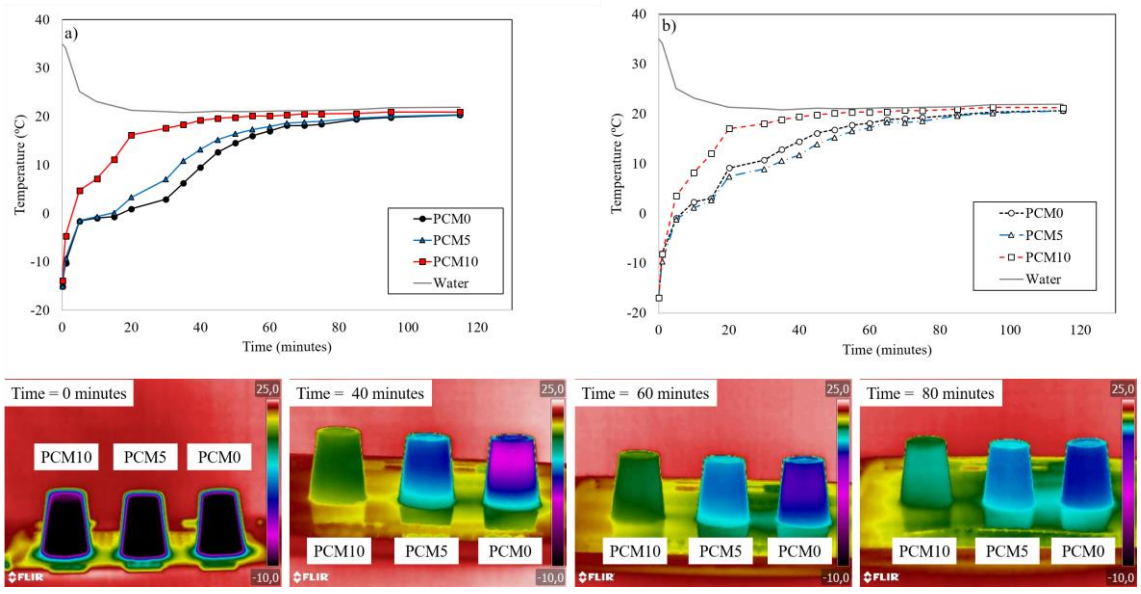

Figure 13. Average temperature variation (n = 3) recorded at heights of 5 cm (a) and 2 cm (b) above the base of the mortar sample during the hot conductivity test, as well as the average temperature variation of the water in contact with the samples. Thermal images of the front sides of the mortar samples, both without and with PCM, at different time intervals are also shown.

4. Conclusions

The main conclusion to be drawn from this study is that addition of this paraffinic PCM (RT 35 HC) to the lime mortar composition decreases, at the same water content, the mortars' accessible porosity, mainly doing so by filling the pores with the smallest diameters. This slows down the carbonation process and increases resistance to the

damage caused by the ingress of external alteration agents, such as water and soluble salts.

Likewise, the reduction in porosity improves the mortar's mechanical resistance, both to impact and compression, by reducing voids and increasing the mechanically useful section.

In addition, the presence of this PCM improves the thermal properties of the mortar, both as regards energy storage and as regards energy transfer. Furthermore, at low temperatures at which the PCM does not reach its melting point its presence increases thermal diffusivity by reducing the number of voids and favoring saturation of the material by capillarity.

This PCM is stable over time; however, a high concentration of this type of PCM causes internal stresses during the thermal melting–solidification cycles due to the different coefficients of thermal expansion between the mortar and the PCM. This offers a real opportunity for energy saving in buildings, although application must be analyzed on a case-by-case basis since it can cause structural damage.

All these changes are more noticeable when larger amounts of the PCM are added to the blend.

This paper contributes to existing knowledge on the direct addition of organic PCMs to lime mortars, which are usually applied in restoration of buildings catalogued as cultural heritage.

Funding

This research was funded by the Autonomous Region of Madrid's Top Heritage Program (S2018/NMT-4372).

Acknowledgments

Special acknowledgment is given to the professional support provided by the Interdisciplinary Thematic Platform at CSIC Open Heritage: Research and Society (PTI-PAIS), and to the Defense University Center at the Spanish Naval Academy (CUD-ENM).

References

[1] UN Environment Programme (UNEP), Global Status Report for Buildings and Construction, 2020.

[2] International Energy Agency, World Energy Outlook, 2020.

[3] C. Alonso, I. Oteiza, J. García-Navarro, F. Martín-Consuegra, Energy consumption to cool and heat experimental modules for the energy refurbishment of façades. Three case studies in Madrid, Energy Build. 126 (2016) 252–262. https://doi.org/https://doi.org/10.1016/j.enbuild.2016.04.034.

[4] R. Vicente, T. Silva, Brick masonry walls with PCM macrocapsules: An experimental approach, Appl. Therm. Eng. 67 (2014) 24–34. https://doi.org/10.1016/J.APPLTHERMALENG.2014.02.069.

[5] N. Zhu, Z. Ma, S. Wang, Dynamic characteristics and energy performance of buildings using phase change materials: A review, Energy Convers. Manag. 50 (2009) 3169–3181. https://doi.org/10.1016/J.ENCONMAN.2009.08.019.

[6] F. Kuznik, J. Virgone, J. Noel, Optimization of a phase change material wallboard for building use, Appl. Therm. Eng. 28 (2008) 1291–1298. https://doi.org/10.1016/J.APPLTHERMALENG.2007.10.012.

[7] A. Nematpour Keshteli, M. Sheikholeslami, Nanoparticle enhanced PCM applications for intensification of thermal performance in building: A review, J. Mol. Liq. 274 (2019) 516–533. https://doi.org/10.1016/J.MOLLIQ.2018.10.151.

[8] M. Frigione, M. Lettieri, A. Sarcinella, Phase change materials for energy efficiency in buildings and their use in mortars, Materials (Basel). 12 (2019). https://doi.org/10.3390/ma12081260.

[9] L.F. Cabeza, A. Castell, C. Barreneche, A. De Gracia, A.I. Fernández, Materials used as PCM in thermal energy storage in buildings: A review, Renew. Sustain. Energy Rev. 15 (2011) 1675–1695. https://doi.org/10.1016/J.RSER.2010.11.018.

[10] T. Yang, W.P. King, N. Miljkovic, Phase change material-based thermal energy storage, Cell Reports Phys. Sci. 2 (2021) 100540. https://doi.org/10.1016/J.XCRP.2021.100540.

[11] M.M. Farid, A.M. Khudhair, S.A.K. Razack, S. Al-Hallaj, A review on phase change energy storage: Materials and applications, Energy Convers. Manag. 45 (2004) 1597–1615. https://doi.org/10.1016/j.enconman.2003.09.015.

[12] R.J. Flatt, N.A. Mohamed, F. Caruso, H. Derluyn, J. Desarnaud, B. Lubelli, R.M. Espinosa- marzal, L. Pel, C. Rodriguez- navarro, G.W. Scherer, N. Shahidzadeh, M. Steiger, Predicting salt damage in practice: a theoretical insight into laboratory tests, RILEM Tech. Lett. 2 (2017) 108–118. https://doi.org/10.21809/rilemtechlett.2017.41.

[13] G.W. Scherer, Crystallization in pores, Cem. Concr. Res. 29 (1999) 1347–1358. https://doi.org/10.1016/S0008-8846(99)00002-2.

[14] A.E. Charola, Salts in the Deterioration of Porous Materials: An Overview, J. Am. Inst. Conserv. 39 (2000) 327–343. https://doi.org/10.1179/019713600806113176.

[15] A.E. Charola, C. Bläuer, Salts in Masonry: An Overview of the Problem, Restor. Build. Monum. 21 (2015) 119–135. https://doi.org/doi:10.1515/rbm-2015-1005.

[16] I. de Rosario, T. Rivas, G. Buceta, J. Feijoo, M.J. Mosquera, Surfactant-Synthesized Consolidants Applied To A Granitic Medieval Necropolis In NW Spain. Laboratory And In Situ Effectiveness Evaluation, Int. J. Archit. Herit. 11 (2017) 1166–1176. https://doi.org/10.1080/15583058.2017.1354097.

[17] I. De Rosario, F. Elhaddad, A. Pan, R. Benavides, T. Rivas, M.J. Mosquera, Effectiveness of a novel consolidant on granite: Laboratory and in situ results, Constr. Build. Mater. 76 (2015) 140–149. https://doi.org/10.1016/J.CONBUILDMAT.2014.11.055.

[18] A.M. Khudhair, M.M. Farid, A review on energy conservation in building applications with thermal storage by latent heat using phase change materials, Energy Convers. Manag. 45 (2004) 263–275. https://doi.org/10.1016/S0196-8904(03)00131-6.

[19] Y. Konuklu, M. Ostry, H.O. Paksoy, P. Charvat, Review on using microencapsulated phase change materials (PCM) in building applications, Energy Build. 106 (2015) 134–155. https://doi.org/10.1016/J.ENBUILD.2015.07.019.

[20] A. D'Alessandro, A.L. Pisello, C. Fabiani, F. Ubertini, L.F. Cabeza, F. Cotana, Multifunctional smart concretes with novel phase change materials: Mechanical and thermo-energy investigation, Appl. Energy. 212 (2018) 1448–1461. https://doi.org/10.1016/J.APENERGY.2018.01.014.

[21] D.W. Hawes, D. Banu, D. Feldman, Latent heat storage in concrete. II, Sol. Energy Mater. 21 (1990) 61–80. https://doi.org/10.1016/0165-1633(90)90043-Z.

[22] D. Zhou, C.Y. Zhao, Y. Tian, Review on thermal energy storage with phase change

materials (PCMs) in building applications, Appl. Energy. 92 (2012) 593–605. https://doi.org/10.1016/J.APENERGY.2011.08.025.

[23] P. Kulkarni, A. Muthadhi, Thermal energy storage cement mortar with direct incorporation of organic and inorganic phase change materials, Innov. Infrastruct. Solut. 6 (2021). https://doi.org/10.1007/S41062-020-00399-4.

[24] J. Feijoo, L.M. Ottosen, X.R. Nóvoa, T. Rivas, I. de Rosario, An improved electrokinetic method to consolidate porous materials, Mater. Struct. 50 (2017). https://doi.org/10.1617/s11527-017-1063-1.

[25] J. Feijoo, R. Fort, L.S. Gomez-Villalba, M.E. Rabanal, L.M. Ottosen, Electroprecipitation of Magnesium and Calcium Compounds for Weathering Protection of Ornamental Rocks, Cryst. Growth Des. 20 (2020) 2337–2355. https://doi.org/10.1021/acs.cgd.9b01497.

[26] S.S. Lucas, V.M. Ferreira, J.L.B. De Aguiar, Latent heat storage in PCM containing mortars - Study of microstructural modifications, Energy Build. 66 (2013) 724–731. https://doi.org/10.1016/j.enbuild.2013.07.060.

[27] L. Ventolà, M. Vendrell, P. Giraldez, Newly-designed traditional lime mortar with a phase change material as an additive, Constr. Build. Mater. 47 (2013) 1210–1216. https://doi.org/10.1016/J.CONBUILDMAT.2013.05.111.

[28] T. Lecompte, P. Le Bideau, P. Glouannec, D. Nortershauser, S. Le Masson, Mechanical and thermo-physical behaviour of concretes and mortars containing phase change material, Energy Build. 94 (2015) 52–60. https://doi.org/10.1016/j.enbuild.2015.02.044.

[29] S. Cunha, J.B. Aguiar, V.M. Ferreira, A. Tadeu, Influence of the type of phase change materials microcapsules on the properties of lime-gypsum thermal mortars,

Adv. Eng. Mater. 16 (2014) 433–441. https://doi.org/10.1002/ADEM.201300278.

[30] S. Cunha, J. Aguiar, F. Pacheco-Torgal, Effect of temperature on mortars with incorporation of phase change materials, Constr. Build. Mater. 98 (2015) 89–101. https://doi.org/10.1016/j.conbuildmat.2015.08.077.

[31] S. Cunha, J.B. Aguiar, A. Tadeu, Thermal performance and cost analysis of mortars made with PCM and different binders, Constr. Build. Mater. 122 (2016) 637–648. https://doi.org/10.1016/j.conbuildmat.2016.06.114.

[32] S. Cunha, P. Leite, J. Aguiar, Characterization of innovative mortars with direct incorporation of phase change materials, J. Energy Storage. 30 (2020) 101439. https://doi.org/10.1016/J.EST.2020.101439.

[33] S. Cunha, M. Lima, J.B. Aguiar, Influence of adding phase change materials on the physical and mechanical properties of cement mortars, Constr. Build. Mater. 127 (2016) 1–10. https://doi.org/10.1016/j.conbuildmat.2016.09.119.

[34] K. Elert, C. Rodriguez-navarro, E. Sebastia, E. Hansen, O. Cazalla, Lime Mortars for the Conservation of Historic Buildings, Stud. Conserv. 47 (2002) 62–75.

[35] L. Ventolà, M. Vendrell, P. Giraldez, L. Merino, Traditional organic additives improve lime mortars: New old materials for restoration and building natural stone fabrics, Constr. Build. Mater. 25 (2011) 3313–3318. https://doi.org/10.1016/J.CONBUILDMAT.2011.03.020.

[36] UNE-EN 459-1:2016, Building lime - Part 1: Definitions, specifications and conformity criteria, (n.d.).

[37] ASTM C144, Standard Specification for Aggregate for Masonry Mortar., (2004).

[38] A. Frazzica, V. Brancato, V. Palomba, D. La Rosa, F. Grungo, L. Calabrese, E.

Proverbio, Thermal performance of hybrid cement mortar-PCMs for warm climates application, Sol. Energy Mater. Sol. Cells. 193 (2019) 270–280. https://doi.org/10.1016/j.solmat.2019.01.022.

[39] UNE-EN 12350-2:2009, Testing fresh concrete – Part 2: Slump-test, (n.d.).

[40] UNE-EN 1936:2007, Natural stone test methods - Determination of real density and apparent density, and of total and open porosity, (n.d.).

[41] UNE-EN 1925:1999, Natural stone test methods - Determination of water absorption coefficient by capillarity, (n.d.).

[42] A. Bernabeu, E. Expósito, V. Montiel, S. Ordóñez, A. Aldaz, A new electrochemical method for consolidation of porous rocks, Electrochem. Commun. 3 (2001) 122–127. https://doi.org/https://doi.org/10.1016/S1388-2481(01)00117-5.

[43] J. Feijoo, L.M. Ottosen, J.S. Pozo-Antonio, Influence of the properties of granite and sandstone in the desalination process by electrokinetic technique, Electrochim. Acta. 181 (2015) 280–287. https://doi.org/10.1016/J.ELECTACTA.2015.06.006.

[44] J. Guyader, A. Denis, Propagation des ondes dans les roches anisotropes sous contrainte évaluation de la qualité des schistes ardoisiers, Bull. Int. Assoc. Eng. Geol. - Bull. l'Association Int. Géologie l'Ingénieur. 33 (1986) 49–55. https://doi.org/10.1007/BF02594705.

[45] D. Costa, A. Magalhães, M. do Rosário Veiga, Characterisation of Mortars Using Drilling Resistance Measurement System (DRMS): Tests on Field Panels Samples, in: J. Válek, J.J. Hughes, C.J.W.P. Groot (Eds.), Hist. Mortars, Springer Netherlands, Dordrecht, 2012: pp. 413–423.

[46] ASTMD 5873:2000, Standard Test Method for Determination of Rock Hardness

by Rebound Hammer Method, (n.d.).

[47] A. Hisashi, Y. Matsukura, Estimating the unconfined compressive strength of intact rocks from Equotip hardness, Bull. Eng. Geol. Environ. 67 (2008) 23–29. https://doi.org/10.1007/s10064-007-0116-z.

[48] S. Ordóñez, R. Fort, M.A. Garcia del Cura, Pore size distribution and the durability of a porous limestone, Q. J. Eng. Geol. 30 (1997) 221–230. https://doi.org/10.1144/GSL.QJEG.1997.030.P3.04.

[49] D. Benavente, M.A.G. del Cura, R. Fort, S. Ordónez, Durability estimation of porous building stones from pore structure and strength, Eng. Geol. 74 (2004) 113–127. https://doi.org/10.1016/J.ENGGEO.2004.03.005.

[50] D. Ergenç, R. Fort, A. Santos Silva, R. Veiga, D. Sanz Arauz, The effects of DiloCarB as carbonation accelerator on the properties of lime mortars, Mater. Struct. 51 (2018). https://doi.org/10.1617/s11527-018-1140-0.

[51] UNE-EN 16140:2019, Natural stone test methods - Determination of sensitivity to changes in appearance produced by thermal cycles, (n.d.).

[52] UNE-EN 12371:2011, Natural stone test methods. Determination of frost resistance, (n.d.).

[53] R.-R.I. des Laboratoiresd'Essaiset, de recherche sur les materiauxet les C. (RILEM), Crystallization test by total immersion (Test V. 1.). Crystallization test by partial immersion (Test V.2.). In: Proceedings of the international symposium deterioration and conservation of stone monuments. UNESCO-RILEM, Paris, (1978).

[54] T. Rivas-Brea, B. Prieto-Lamas, B. Silva-Hermo, Artificial weathering test of granitic rocks, Mater. Constr. 58 (2008) 179–189.

https://doi.org/10.3989/mc.2008.v58.i289-290.80.

[55] B. Silva, T. Rivas, E. García-Rodeja, B. Prieto, Distribution of ions of marine origin in Galicia (NW Spain) as a function of distance from the sea, Atmos. Environ. 41 (2007) 4396–4407. https://doi.org/10.1016/J.ATMOSENV.2007.01.045.

[56] B. Silva, T. Rivas, B. Prieto, Soluble salts in granitic monuments: origin and decay effects, Appl. Study Cult. Herit. Clays. (2003) 113–130.

[57] A.E. Charola, J. Pühringer, M. Steiger, Gypsum: a review of its role in the deterioration of building materials, Environ. Geol. 52 (2007) 339–352. https://doi.org/10.1007/s00254-006-0566-9.

[58] N. Tsui, R.J. Flatt, G.W. Scherer, Crystallization damage by sodium sulfate, J. Cult. Herit. 4 (2003) 109–115. https://doi.org/10.1016/S1296-2074(03)00022-0.

[59] J. Feijoo, L.M. Ottosen, O. Matyscak, R. Fort, Electrokinetic desalination of a farmhouse applying a proton pump approach. First in situ experience, Constr. Build. Mater. 243 (2020). https://doi.org/10.1016/j.conbuildmat.2020.118308.

[60] J. Feijoo, T. Rivas, X.R. Nóvoa, I. de Rosario, J. Otero, In situ desalination of a granitic column by the electrokinetic method, Int. J. Archit. Herit. 12 (2018) 63–74. https://doi.org/10.1080/15583058.2017.1370509.

[61] J. Feijoo, X.R. Nóvoa, T. Rivas, M.J. Mosquera, J. Taboada, C. Montojo, F. Carrera, Granite desalination using electromigration. Influence of type of granite and saline contaminant, J. Cult. Herit. 14 (2013) 365–376. https://doi.org/10.1016/J.CULHER.2012.09.004.

[62] R. Fort, J. Feijoo, M.J. Varas-Muriel, M.A. Navacerrada, M.M. Barbero-Barrera, D. De la Prida, Appraisal of non-destructive in situ techniques to determine

moisture- and salt crystallization-induced damage in dolostones, J. Build. Eng. 53 (2022). https://doi.org/https://doi.org/10.1016/j.jobe.2022.104525.

[63] F. Rebelo, A. Figueiredo, R. Vicente, V.M. Ferreira, Study of a thermally enhanced mortar incorporating phase change materials for overheating reduction in buildings, J. Energy Storage. 46 (2022). https://doi.org/10.1016/j.est.2021.103876.

[64] M.T. Marvila, A.R.G. Azevedo, S.N. Monteiro, Verification of the application potential of the mathematical models of lyse, abrams and molinari in mortars based on cement and lime, J. Mater. Res. Technol. 9 (2020) 7327–7334. https://doi.org/10.1016/j.jmrt.2020.04.077.

[65] Z. Pavlík, A. Trník, J. Ondruška, M. Keppert, M. Pavlíková, P. Volfová, V. Kaulich, R. Černý, Apparent thermal properties of phase-change materials: An analysis using differential scanning calorimetry and impulse method, Int. J. Thermophys. 34 (2013) 851–864. https://doi.org/10.1007/s10765-012-1169-1.

[66] B. Meng, Calculation of moisture transport coefficients on the basis of relevant pore structure parameters, Mater. Struct. 27 (1994) 125–134. https://doi.org/10.1007/BF02473025.

[67] R. Fort, M.J. Varas, M. Alvarez de Buergo, D. Martin-Freire, Determination of anisotropy to enhance the durability of natural stone, J. Geophys. Eng. 8 (2011) S132–S144. https://doi.org/10.1088/1742-2132/8/3/S13.

[68] L.M.O. Sousa, L.M. Suárez del Río, L. Calleja, V.G. Ruiz de Argandoña, A. Rodríguez Rey, Influence of microfractures and porosity on the physico-mechanical properties and weathering of ornamental granites, Eng. Geol. 77 (2005) 153–168. https://doi.org/10.1016/J.ENGGEO.2004.10.001.

[69] J. Feijoo, X.R. Nóvoa, T. Rivas, Electrokinetic treatment to increase bearing

capacity and durability of a granite, Mater. Struct. 50 (2017). https://doi.org/10.1617/s11527-017-1123-6.

[70] K. Beck, M. Al-Mukhtar, Formulation and characterization of an appropriate lime-based mortar for use with a porous limestone, Environ. Geol. 56 (2008) 715–727. https://doi.org/10.1007/s00254-008-1299-8.

[71] A. La Iglesia, V. González, V. López-Acevedo, C. Viedma, Salt crystallization in porous construction materials I Estimation of crystallization pressure, J. Cryst. Growth. 177 (1997) 111–118. https://doi.org/10.1016/S0022-0248(96)01072-X.

[72] D. Ergenç, J. Feijoo, R. Fort, M. Alvarez de Buergo, Effects of potassium ferrocyanide used for desalination on lime composite performances in different curing regimes, Constr. Build. Mater. 259 (2020) 120409. https://doi.org/10.1016/J.CONBUILDMAT.2020.120409.

[73] H. Paiva, A. Velosa, R. Veiga, V.M. Ferreira, Effect of maturation time on the fresh and hardened properties of an air lime mortar, Cem. Concr. Res. 40 (2010) 447–451. https://doi.org/10.1016/j.cemconres.2009.09.016.

[74] T.W. Chen, J. Wu, G.Q. Dong, Mechanical properties and uniaxial compression stress—strain relation of recycled coarse aggregate concrete after carbonation, Materials (Basel). 14 (2021). https://doi.org/10.3390/ma14092215.

[75] J. Lanas, J.I. Alvarez-Galindo, Masonry repair lime-based mortars: factors affecting the mechanical behavior, Cem. Concr. Res. 33 (2003) 1867–1876. https://doi.org/https://doi.org/10.1016/S0008-8846(03)00210-2.

[76] B.A. Güney, E. Caner, Thermal and hygric expansion characteristics of mortars and bricks used in the dome structures of Turkish Baths from 14th and 15th centuries, Constr. Build. Mater. 95 (2015) 757–761.

https://doi.org/https://doi.org/10.1016/j.conbuildmat.2015.07.176.

[77] T. Diaz Gonçalves, V. Brito, Differential thermal expansion as a cause of salt decay: literature review, experiments, and modelling of micro and macro effects on Ançã limestone, Stud. Conserv. 62 (2017) 310–328. https://doi.org/10.1080/00393630.2016.1140860.

[78] B.A. Young, Z. Wei, J. Rubalcava-Cruz, G. Falzone, A. Kumar, N. Neithalath, G. Sant, L. Pilon, A general method for retrieving thermal deformation properties of microencapsulated phase change materials or other particulate inclusions in cementitious composites, Mater. Des. 126 (2017) 259–267. https://doi.org/10.1016/j.matdes.2017.04.023.

[79] J. Feijoo, I. de Rosario, T. Rivas, M.J. Mosquera, R. Benavides, Influence of a Pre-consolidation Treatment on the Desalination Effectiveness of a Highly Deteriorated Granite Façade of Medieval Age, Int. J. Archit. Herit. 0 (2022) 1–19. https://doi.org/10.1080/15583058.2022.2086506.

[80] T. Salgueiro, A. Samagaio, M. Gonçalves, A. Figueiredo, J. Labrincha, L. Silva, Incorporation of phase change materials in an expanded clay containing mortar for indoor thermal regulation of buildings, J. Energy Storage. 36 (2021) 102385. https://doi.org/https://doi.org/10.1016/j.est.2021.102385.

[81] P. Shafigh, I. Asadi, A.R. Akhiani, N.B. Mahyuddin, M. Hashemi, Thermal properties of cement mortar with different mix proportions, Mater. Constr. 70 (2020) 1–12. https://doi.org/10.3989/mc.2020.09219.

[82] R. Jorand, A. Fehr, A. Koch, C. Clauser, Study of the variation of thermal conductivity with water saturation using nuclear magnetic resonance, J. Geophys. Res. 116 (2011) 8208. https://doi.org/10.1029/2010JB007734.

Declaration of interests

☒The authors declare that they have no known competing financial interests or personal relationships that could have appeared to influence the work reported in this paper.

☐The authors declare the following financial interests/personal relationships which may be considered as potential competing interests: